Available online at www.sciencedirect.com
ScienceDirect
Tunnelling and Underground Space Technology 22 (2007) 620–632
Tunnelling and Underground Space Technology incorporating Trenchless Technology Research
www.elsevier.com/locate/tust

Stability analysis of a borehole wall during horizontal directional drilling

X. Wang *, R.L. Sterling

Trenchless Technology Center, Louisiana Tech University, Ruston, LA 71272, United States

Available online 28 February 2007

Abstract

In this paper, numerical simulation strategies are proposed and numerical analyses are performed to investigate the stability of a borehole wall during horizontal directional drilling in loose sand with an emphasis on the role of the filter cake in borehole stability. Two computational scenarios, one in the absence of a filter cake and one with the presence of a filter cake in a borehole wall, are investigated by considering both deep and shallow borehole situations. In the case where no filter cake is formed, the soil–drilling fluid interaction analysis shows that the effective pressure on soil particles will quickly decrease to zero even at a low drilling fluid pressure because of the rapid drainage of the drilling fluids into the loose sands. This conforms to the classical liquefaction criterion, indicating that static (flow) liquefaction-based soil crumbling and sloughing will occur even at a very low drilling fluid pressure if an effective filter cake is not formed. Soil's permeability effect on pore pressure and the transition to a steady flow are also studied. In the second scenario in which a filter cake is formed, the hydraulic fracture failures around the bores are investigated, which are caused by the expansion of the yielding zones. The yield zone sizes and critical drilling fluid pressures at the moment of hydraulic fracturing failure are calculated from the finite element analyses and the closed-form solution, which is based on classical plasticity theories. The critical fluid pressures from the finite element analyses and the closed-form solutions are very close, but there is a large discrepancy between the yield zone sizes.
Published by Elsevier Ltd.

Keywords: Stability analysis; Horizontal directional drilling; Finite element method; Filter cake; Soil and drilling fluid coupling; Critical drilling fluid pressure

1. Introduction

Horizontal directional drilling (HDD) is a trenchless construction method typically used for the installation of small-to-medium sized pipelines and conduits at relatively shallow depths by using a surface-mounted rig (Bennett et al., 1995; Marshall et al., 2001). In the last 10 years, with the improvement of HDD techniques, it has become a popular and increasingly viable method for infrastructure installation in different areas within the construction industry, such as natural gas, electrical power and communication industries (Chevron Chemical Co., LLC, 1999; Conroy et al., 2002; Latorre et al., 2002). In horizontal directional drilling practice, the first step is to drill a guided pilot hole along the bore path consisting of a shallow arc by mechanically cutting and mixing soil and/or rock formations with drilling fluids to form a flowable slurry. In the second or subsequent step(s), the bore is sufficiently enlarged with larger diameter back reamer(s) before the product pipe is pulled into the bore and installed in the subsurface (Ariaratnam and Lueke, 2002).

Despite its popularity and success, a number of issues relating to the HDD installation remain poorly understood. One of the important issues, concerning the application of HDD to very loose sand or gravel–sand mixtures, and presenting a big challenge to HDD industry, is how to effectively evaluate the stability of the borehole wall. Borehole collapse can lead to drill rods or pipes becoming stuck in the borehole and borehole fracture can result in the release of drilling fluids from the borehole. To date,

* Corresponding author. Tel.: +1 318 257 2934; fax: +1 318 257 2306.
E-mail address: xwang@latech.edu (X. Wang).

0886-7798/$ - see front matter Published by Elsevier Ltd.
doi:10.1016/j.tust.2007.01.002

some empirical equations based on the classical plasticity theory are employed to calculate the critical fluid pressures to prevent the borehole from collapse and hydraulic fracture in HDD practice (Staheli et al., 1998). It should also be noted that while borehole stability has been extensively studied in the petroleum exploration industry, the conditions under which borehole stability are investigated are very different from the conditions for horizontal directional drilling. In the former, stability has been studied principally in vertical boreholes at great depth in rock. In the latter, the stability of horizontal boreholes at relatively shallow depths in loose soils is the issue.

In this paper, the borehole stability problem, from the collapse of granular soils near the borehole wall to the hydraulic fracturing induced by high drilling mud pressure, will be studied using the finite element method. Unlike closed-form analytical formulae that are based on the classic rigid-perfect plasticity theories or the empirical equations dependent on statistical analyses for computations of the stresses near the horizontal borehole, the numerical model can easily integrate specific elasto-plastic constitutive descriptions (strain hardening and softening, and failure modes), inhomogeneities, and anisotropies of soils. The in-situ earth pressure will be reasonably accounted for prior to the construction of the horizontal directional drilling, and the sequential construction procedures (excavation of the pilot hole and back reaming, etc.) will be incorporated in the elasto-plastic model to get realistic stress distributions. Elasto-plastic analyses of the filter cake and the soil mass will give the minimum and maximum drilling fluid pressures to avoid the development of large plastic yield zones and the initiation of hydraulic fracturing or tensile rupture, which may eventually lead to drilling fluid circulation loss (Wang and Dusseault, 1991; Wang et al., 1994).

Using advanced simulation techniques, the importance of creating a filter cake will be studied by coupling the mechanics of the soil and drilling fluid interactions. The criterion for soil instability and soil sloughing will be associated with the fluid behavior of loose sand, defined as soil liquefaction and commonly referred to as "quicksand" (Hair, 1995a,b). The filter cake, which plays an important role in preventing borehole instability, involves the interaction between soil mass, flowing slurry, and ground water.

In this paper, an appropriate elasto-plastic soil constitutive model is used to reflect the soil deformation properties and failure modes. Static (flow) liquefaction, initiation and development of a plastic yielding zone, and the hydraulic fracture in the borehole wall are modeled to evaluate the borehole stability. The research is intended to develop an efficient numerical strategy to provide quantitative estimates for the safe range of drilling pressures for various site conditions and borehole depths, and also to develop a quantitative understanding about the role of a filter cake in borehole stability. The research uses well-documented soil constitutive models and broadly accepted cutting-edge numerical tools. This paper provides the results of some initial simulations of the problem; an ongoing research program is planned to further refine simulation techniques and the understanding of the physical interactions occurring at the borehole wall.

2. A brief description of the theoretical bases of the analyses

Borehole stability requires a proper balance among various soil parameters including: soil stress and strength, pore pressure, drilling fluid pressure and drilling mud chemical composition. Borehole instability is influenced by chemical effects (formation of a filter cake) and mechanical effects (soil sloughing and hydraulic fracturing). The finite element method is the fundamental tool to be used for the establishment of the analysis system in this research. Existing analytical solutions for horizontal boreholes have been published and implemented in some design tools for industry application, which are based on the classical rigid-perfect plasticity theories (Chevron Chemical Co., LLC, 1999; Conroy et al., 2002). Recently, numerical methods have also been used to investigate borehole stability in HDD. Duyvestyn and Knight (2000) applied the finite difference method (commercial software FLAC) to predict soil deformations due to horizontal directional drilling pipeline installation. The finite element method presented in this paper provides a state-of-the-art poro-mechanical approach to account for effects of coupled diffusion/deformation, which is governed by an equation that describes how total strains of the porous soil depend on the total applied stresses and pore pressure weighted by Biot's effective stress parameter (Biot, 1956, 1977). In this parameter, the pore pressure is related to the pore fluid content variation, as well as the deformation of the porous body. Commercial finite element software ADINA (2001) is employed to carry out the numerical analyses.

2.1. Constitutive modeling of the granular soil mass

In order to perform the borehole wall stability analysis, the granular soil deformation and strength behaviors such as yielding, perfect plasticity, strain hardening and failure modes involving the pressure-enhanced shear strength at different loading conditions should be correctly characterized in their constitutive descriptions (Desai and Christian, 1977). In this paper, the Drucker–Prager model will be employed. The corresponding material parameters will be obtained from the conventional triaxial compression or extension test data. Based on the elasto-perfectly plastic stress–strain relationship, the yield function of the Drucker–Prager model is written as follows (Chen and Mizuno, 1990):

$$f = \alpha I_1 + \sqrt{J_2} - \kappa = 0 \tag{1}$$

in which I_1 and J_2 represent the first stress invariant and the second deviatoric stress invariant, respectively. If the Drucker–Prager circle coincides with the outer apices of the Mohr–Coulomb hexagon, we can have

$$\alpha = \frac{2\sin\phi}{\sqrt{3}(3-\sin\phi)}, \quad \kappa = \frac{6c\cos\phi}{\sqrt{3}(3-\sin\phi)} \tag{2}$$

where ϕ is the internal frictional angle. With ϕ replaced by the dilatational angle ψ for the associated flow rule, a plastic potential function can be established for the Drucker–Prager model.

2.2. The coupled analysis of drilling fluid and soil mass – a generalized fluid–structure interaction model

During the drilling of a pilot hole and the subsequent back reamed hole, drilling fluids are normally injected in the borehole to stabilize the bore, carry the fragmented soil wastes and lubricate the pipe and drill-string, etc. The drilling fluid, flowing through the annular space between the drill rod or pipeline and the borehole wall, and seeping into the borehole wall, interacts with the surrounding soil and ground water, mechanically, thermally and chemically. The chemical and mechanical interaction between the drilling fluid and soil will give rise to the possible swift formation of the so-called filter cake, which plays a crucial role for the borehole stability. The filter cake will prevent the drilling fluid from seeping further into ground surrounding the borehole wall. To make the interaction modeling simple, the chemical interaction leading to the formation of the filter cake will be ignored here. The possible temperature difference between the drilling fluid and the soil mass is also neglected in this research. The effective stresses (pressure acting on soil particles, normal and shear stresses) change near the borehole because the mechanical interaction will cause the soil mass near the borehole to experience a decrease in its shear strength. If the residual strength is low enough because of the increase in pore pressure, static (flow) liquefaction will occur in the soil, which will cause the soil to slough or crumble. Eventually, the hole will probably collapse. The analysis of unstable soil sloughing will provide the minimum drilling fluid pressure and the required properties of the filter cake to support loose soil grains. If the drilling fluid pressure is too high, a large plastic yield zone and hydraulic fracturing will develop from the borehole boundary and propagate into the deep borehole wall. This may eventually lead to collapse of the borehole wall and to drilling fluid circulation loss. In order to provide quantitative estimates for the safe range of drilling pressures, and also to gain a deeper understanding of the role of the filter cake in providing borehole stability, numerical analyses of two scenarios are performed. In the first scenario, where an effective filter cake is not formed, drilling fluids will keep seeping into a soil mass, which has high permeability. For this scenario, a fully coupled analysis of the soil medium and drilling fluids will be considered. In the poro-mechanical model used, displacement is an independent variable at each nodal point, and pore fluid pressure is the second independent variable at each corner nodal point (Wang and Dong, 2003). In the second scenario, a filter cake is formed before the drilling fluids flow extensively into the borehole wall and the filter cake is assumed to prevent the further seepage of the drilling fluids during the drilling period. For this scenario, a pure elasto-plastic analysis without coupling is performed.

3. Scenarios of the numerical simulations

In order to obtain a precise and useful solution, the flow of drilling fluid through the drill pipe annulus should be considered. Based on the recent development of computational mechanics, the drilling flow through the annular space can be modeled in connection with the pore flow through the bore wall (Bathe et al., 1999; Zhang et al., 2003). Two 2-D analyses are performed, one covers the longitudinal sectional area of the borehole, and the other one is for the cross-sectional area of the borehole.

Results presented in this paper, however, are only for the simplified case where the drilling fluid behavior is simulated by applying a fluid pressure on the cross-sectional boundary of the borehole wall. The interaction is only considered between the pore flow and the porous wall medium.

A conceptual solution procedure is given in this section, which is based on the foregoing framework. An entire computational work is completed in several steps, from which critical drilling fluid pressures are obtained: the lower critical pressure under which soils near a borehole will crumble and which may lead to the collapse of the borehole wall; and an upper critical pressure which induces the inception and propagation of plastic yield zones and hydraulic fractures eventually. In all of the following analyses to be performed, gel strengths of the drilling fluid are assumed large enough to suspend drilled spoil when the fluid is at rest.

The cross-section of a half bore is taken for analysis because of symmetry, as shown in Fig. 1. In the deep bore situation, for demonstration purposes, the borehole is assumed drilled through a very loose natural levee at the depth of 30.48 m with a diameter of 38.1 cm. In the shallow bore situation, a borehole of the same size is drilled through the same soil at the depth of 6.10 m. Mechanical properties of the soil (including the filter cake) are given in Table 1. It should be noted that since the associated flow

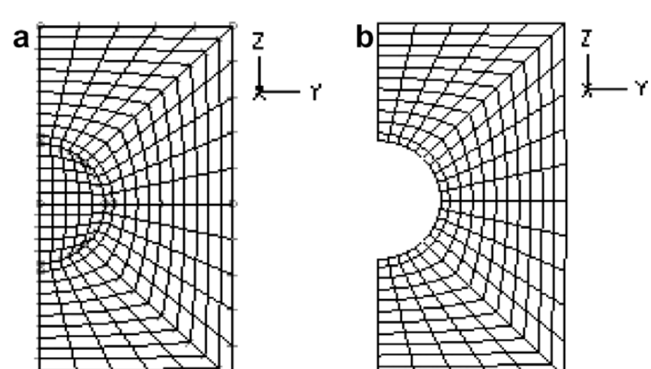

Fig. 1. Mesh discretization around the borehole: (a) before excavation and (b) after excavation.

Table 1
Soil material properties

	Modulus of elasticity (MPa)	Poisson's ratio	Frictional angle (°)	Cohesion (kPa)	Density (kg/m^3)
Soil	69.0	0.35	20	69	1474
Filter cake	138.0	0.35	25	138	1474

rule is used, it is assumed that the angle of dilation is the angle of friction.

The soil mass above the borehole will be meshed all the way up to the ground surface as shown in Figs. 1 and 2. The soil mass is horizontally 12 times as large as the bore radius. The distance from the bottom of the bore to the bottom of the soil mass is 20 times as large as the bore radius. The left and right sides of the soil mass are both pinned horizontally and free for vertical movement, and the bottom boundary is fixed in two directions. The gravity of the soil mass is applied as a body force.

4. Numerical solutions

As described in Section 2, numerical analyses will be performed in two scenarios. Scenario 1: A filter cake is not formed before drilling fluids seep deeply into the borehole wall. In this scenario, a fully two-phase poro-elasto-plastic coupled analysis will be undertaken. Scenario 2: A filter cake is formed with much lower permeability and higher material strength and modulus of elasticity. In this case, the drilling fluid is assumed not to seep into the borehole wall. Only an elasto-plastic analysis is carried out for the soil mass around the borehole. In all the stress solutions shown below, a geotechnical stress sign convention is employed in which compression takes a positive sign and tension a negative sign. However, in the pore pressure distribution plots, positive sign represents tension and negative sign for compression. The analyses for the two scenarios are performed, respectively.

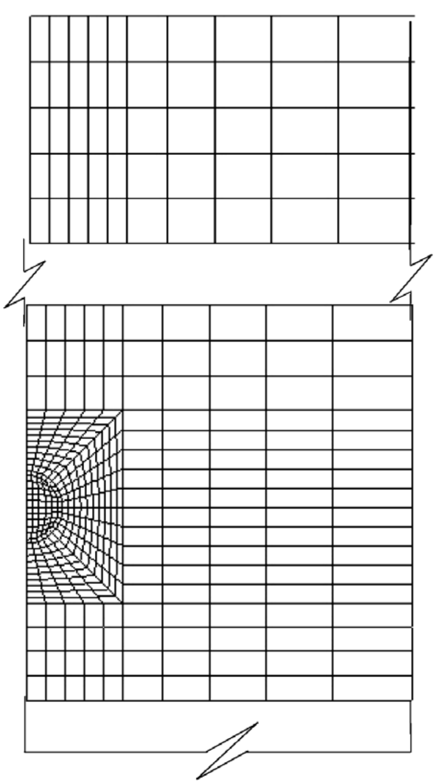

Fig. 2. Mesh discretization of the soil mass around the borehole.

4.1. Scenario one: no filter cake

In the cases of both deep and shallow borehole situations, the soil domains are discretized using a total of 1520 plane strain quadrilateral 9-node solid elements for the discretized domain. Soils through the whole domain are assumed homogeneous. Analyses are conducted for the boreholes at two different overburden depths, which correspond to the drilling fluid pressures on the borehole boundary given in Table 2 (deep hole situation) and Table 3 (shallow hole situation). They remain constant throughout the analyses. Permeability of the soil is identical in the X, Y and Z directions. In this research, two permeabilities, $4.45e^{-11}$ Pa m^2/s and $4.45e^{-6}$ Pa m^2/s, are taken for the soils, respectively. Excess pore pressure is assumed zero on the boundaries of the soil mass except the borehole perimeter where pore pressure is equal to the drilling fluid pressure. All the solutions presented, such as excess pore pressures and pressures between soil particles near the

Table 2a
Minimum soil pressure at the bore crown at the specified drilling fluid pressures (deep hole case, permeability $k = 4.45e^{-11}$ Pa m^2/s)

Drilling fluid pressure (kPa)	165.5	172.4	179.3	186.2	193.1	196.5
Soil pressure (kPa)						
Initial	5.68	1.14	−3.43	−8.01	−12.60	−14.90
Steady	15.60	11.60	7.54	3.52	0.53	−2.56

Table 2b
Minimum soil pressure at the bore crown at the specified drilling fluid pressures (deep bore case, permeability $k = 4.45e^{-6}$ Pa m^2/s)

Drilling fluid pressure (kPa)	172.4	179.3	186.2	193.1	200.0	206.9
Soil pressure (kPa)						
Initial	12.20	8.14	4.13	0	−4.08	−8.15
Steady	11.50	7.49	3.47	−0.57	−4.62	−8.68

Table 3a
Minimum soil pressure at the bore crown at the specified drilling fluid pressures (shallow bore case, permeability $k = 4.45e^{-11}$ Pa m^2/s)

Drilling fluid pressure (kPa)	27.6	34.5	44.1	88.3
Soil pressure (kPa)				
Initial	4.66	−0.06	−6.8	−36.90
Steady	6.46	2.19	−3.80	−31.20

Table 3b
Minimum soil pressure at the bore crown at the specified drilling fluid pressures (shallow bore case, permeability $k = 4.45e^{-6}$ Pa m^2/s)

Drilling fluid pressure (kPa)	27.6	34.5	44.1	88.3
Soil pressure (kPa)				
Initial	6.61	2.38	−3.55	−30.70
Steady	6.62	2.38	−3.55	−30.70

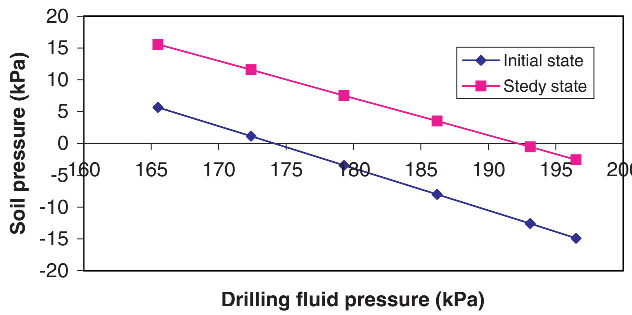

Fig. 3. Drilling fluid pressure versus the minimum soil pressure at the crown (deep bore, permeability $k = 4.45e^{-11}$ m^2 Pa/s).

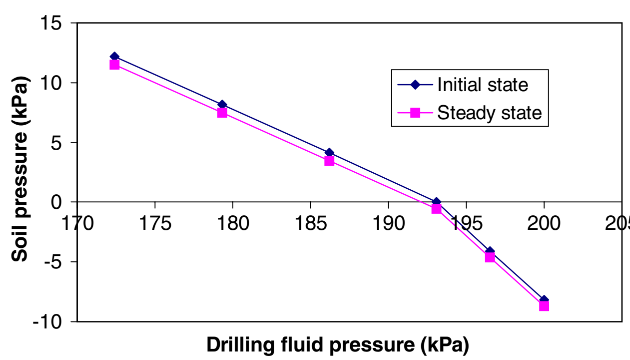

Fig. 4. Drilling fluid pressure versus minimum soil pressure at the borehole crown area (deep bore, permeability $k = 4.45e^{-6}$ Pa m^2/s).

borehole boundary, are time dependent. Increase in pore pressure will decrease the effective stress around the borehole. As a result, it will lead to the reduction of soil strength. Flow liquefaction will be likely to occur in the area. For the sake of simplicity, flow liquefaction is characterized here by the classical liquefaction criterion that the reduction to zero effective stress by induced pore pressure implies the occurrence of liquefaction (Morgenstern, 1994). In this paper, the flow liquefaction is considered to initiate from where the effective soil pressure reduces to zero.

The pore pressures on all the boundaries are time independent. But they are time dependent at any point within the borehole wall domain. For the deep bore case with a depth of 30.48 m, Tables 2a and 2b give the minimum soil pressure values at the bore crowns when the soil permeability is $4.45e^{-11}$ Pa m^2/s and $4.45e^{-6}$ Pa m^2/s, respectively. If the soil has a low permeability, the minimum soil pressure acts on the bore crown immediately after the seepage starts. Then, it will be getting larger and larger before the steady drilling fluid flow is reached. If the soil takes a permeability of $4.45e^{-6}$ Pa m^2/s, Tables 2b and 3b imply that a steady flow in the bore wall is reached very quickly. Under the condition of lower permeability, Fig. 3 also shows the relationship between the drilling fluid pressure and the minimum soil pressure at the bore crown area for the lower permeability situation. It presents nearly a zero soil pressure as soon as the drilling fluid pressure reaches 174 kPa, and the soil pressure will stay at zero after a steady drilling fluid flow is formed at a drilling fluid pressure of 193 kPa. It implies that static soil liquefaction is likely to occur after the drilling fluid pressure arrives at 174 kPa. When the soil permeability takes a value of $4.45e^{-6}$ Pa m^2/s, Fig. 4 shows that the critical drilling fluid pressure will rise to 194 kPa. In the shallow bore case with an overburden depth of 6.1 m, Figs. 9 and 10 give critical

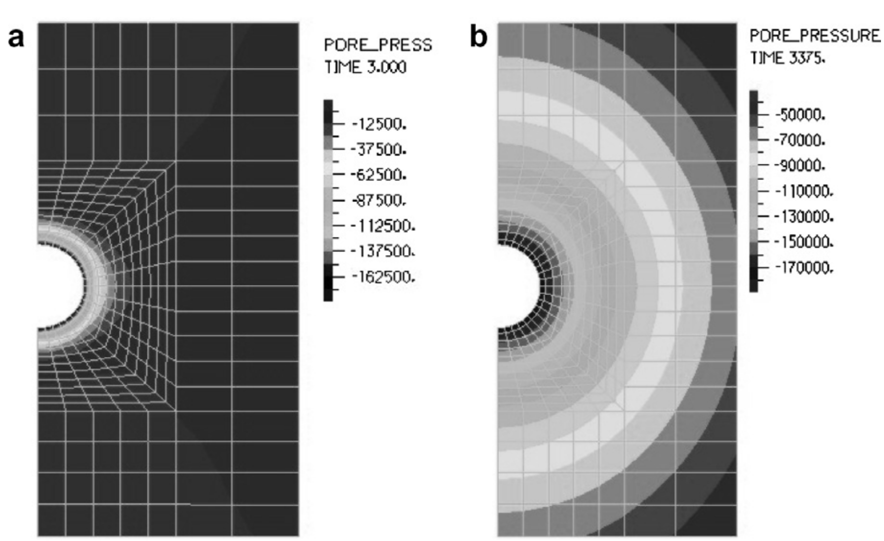

Fig. 5. Initial pore pressure (a) and steady pore pressure (b) distributions around the borehole (deep bore, drilling fluid pressure $p_0 = 179.4$ kPa, permeability $k = 4.45e^{-11}$ Pa m^2/s).

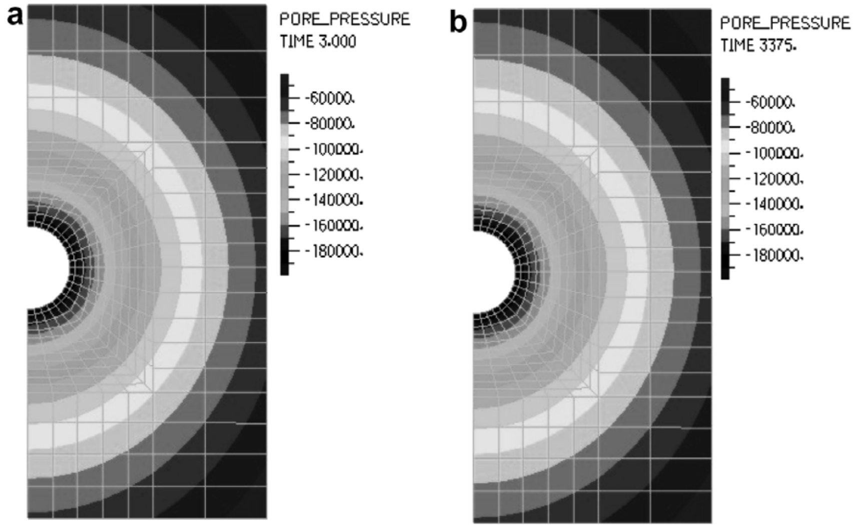

Fig. 6. Initial pore pressure (a) and steady pore pressure (b) distributions around the borehole (deep bore, drilling fluid pressure $p_0 = 193.1$ kPa, permeability $k = 4.45\text{e}^{-6}$ Pa m^2/s).

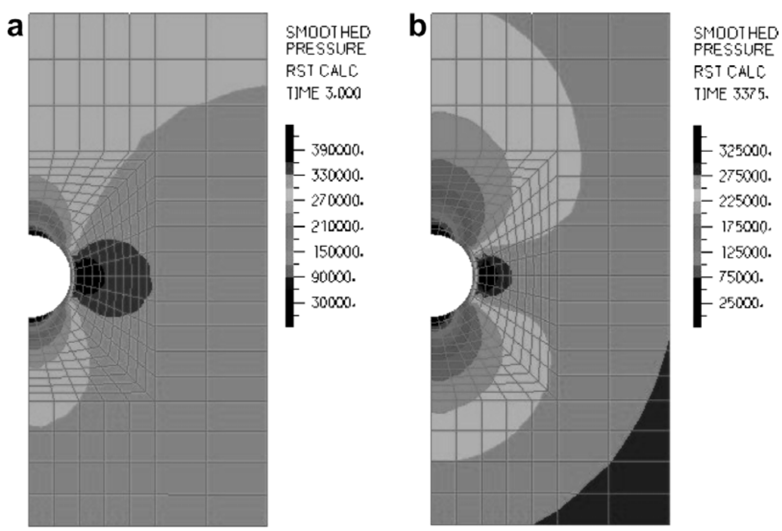

Fig. 7. Soil pressure distribution at the initial flow condition (a) and at the steady flow condition (b) (deep bore, $p_0 = 179.4$ kPa, permeability $k = 4.45\text{e}^{-11}$ Pa m^2/s).

drilling fluid pressures of 33 kPa and 39 kPa for low permeability and high permeability situations, respectively. Representative initial and steady pore pressure distributions around the borehole are given in Figs. 5 and 6 for the deep bore case, and Figs. 11 and 12 for the shallow bore case, respectively. They have shown again that soils with high permeability will have high critical drilling fluid pressure against a static liquefaction-based soil problem like soil crumbling or sloughing. When the permeability increases from 4.45e^{-11} Pa m^2/s to 4.45e^{-6} Pa m^2/s, the steady flow condition will be approached shortly after the bore is drilled. The soil pressure distributions with the initial and steady flow conditions in the same local areas are presented in Figs. 7 and 8 for the deep bore case. Figs. 13 and 14 show the soil pressure distributions for the shallow bore case. The pore pressure and the soil pressure solutions in this research strongly suggest that a filter cake plays an essential role in maintaining bore wall stability. Flow liquefaction-induced soil crumbling, which may result in the collapse of a borehole, is more likely to occur if no filter cake forms around the borehole boundary immediately after the drilling penetration in loose sand.

4.2. Scenario two: existence of a filter cake

With an effective physio-chemical interaction between the drilling fluid and soil, a filter cake may form as quickly as the drilling fluid seeps into the bore wall. A stiffer filter cake, with a much lower permeability and higher shear strength, will prevent the drilling fluids from seeping fur-

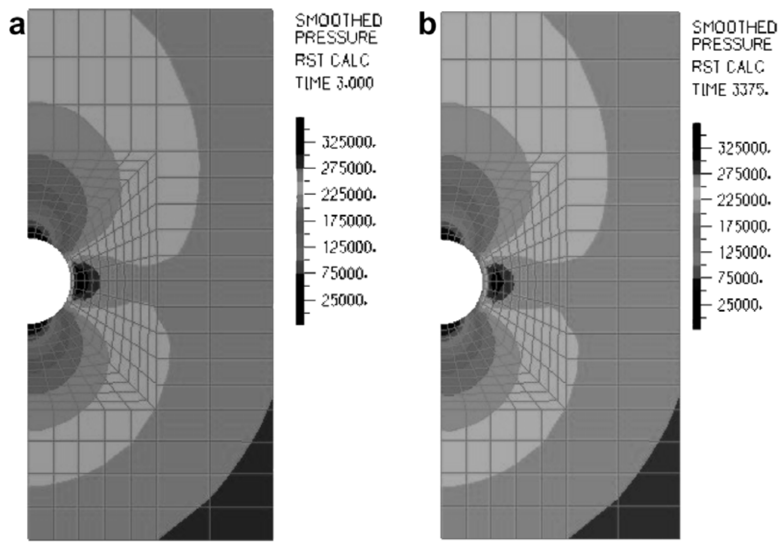

Fig. 8. Soil pressure distributions at the initial flow condition (a) and at the steady flow condition (b) (deep bore, $p_0 = 193.1$ kPa, permeability $k = 4.45e^{-6}$ Pa m^2/s).

ther into the borehole wall. In the corresponding analysis for a limited period of horizontal drilling time, an assumption can be made that no significant seepage effect occurs behind the filter cake. The soil and filter cake are also both modeled using the Drucker–Prager yield criterion with the same or different mechanical properties, as listed in Table 1 for both cases with drilled holes at different depths. The same domain and mesh discretization as used in the first scenario will be applied to the computations at this stage. Based on the research work done by Arends (2003), the filter cake is assumed 2.54 cm thick.

At this stage, the drilling fluid pressure will be gradually increased, as shown in Table 4 for the deep bore situation and Table 5 for the shallow bore situation, respectively. The occurrence and growth of plastic yielding indicate the inception and propagation of the hydraulic fracturing zone in the wall.

In the case of the deep bore, band plots of yield function values are given in Fig. 15, which correspond to the six different drilling fluid pressures. The dark areas around the borehole represent the plastic yield zones.

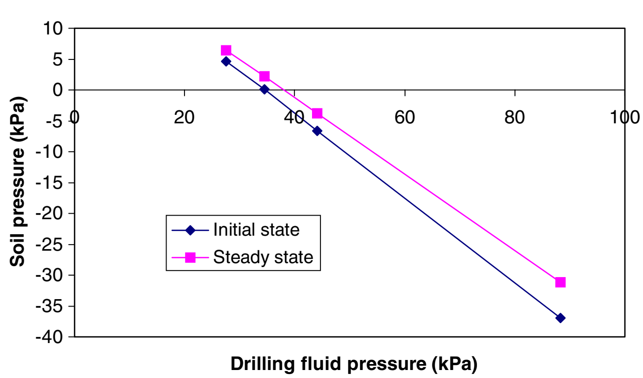

Fig. 9. Drilling fluid pressure versus minimum soil pressure on the bore crown (shallow bore, permeability $k = 4.45e^{-11}$ Pa m^2/s).

Before the drilling fluid pressure is applied, a plastic yield zone has appeared near the springline of the borehole. With an increase in the drilling fluid pressure, the plastic yield zone diminishes. From Fig. 15a, it can be seen that the plastic yield zone dramatically dwindles as the drilling fluid pressure reaches 0.48 MPa, which is nearly equal to the overburden pressure, but new plastic yield zones have developed at the crown and invert areas of the borehole. Nevertheless, the plastic yield zones stay the smallest if the drilling fluid pressure is equal to the overburden earth pressure. With the increase in the drilling fluid pressure, the plastic yield zones expand more and more significantly, as shown in Fig. 15, where red colored yield zones are plotted at different drilling fluid pressures. As the drilling fluid pressure rises to 3.0 MPa, which is around 6.8 times the overburden earth pressure, a broad plastic zone around the borehole has been developed at the crown and invert areas of the borehole wall. The plastic zone is from the crown to the invert, with its radius approximately three times as large as the borehole radius. The fracture failure occurs around the borewall because of the extremely large yield zone at the drilling fluid pressure of 3.0 MPa.

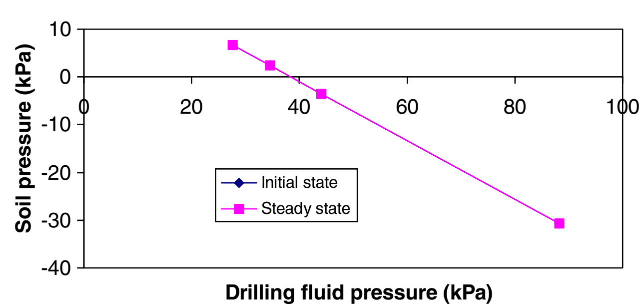

Fig. 10. Drilling fluid pressure versus minimum soil pressure on the bore crown (shallow bore, permeability $k = 4.45e^{-6}$ Pa m^2/s).

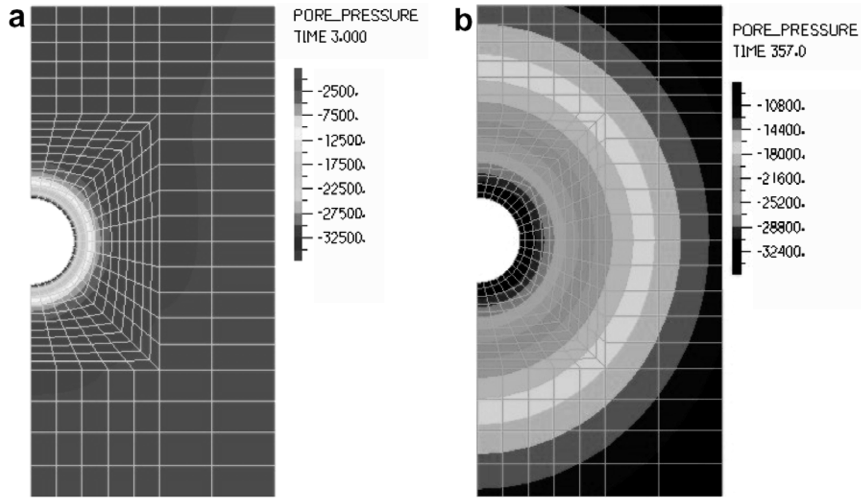

Fig. 11. Pore pressure distribution (shallow bore, $p_0 = 34.5$ kPa, permeability $k = 4.45e^{-11}$ Pa m^2/s) (a) at the initial stage and (b) at the steady flow condition.

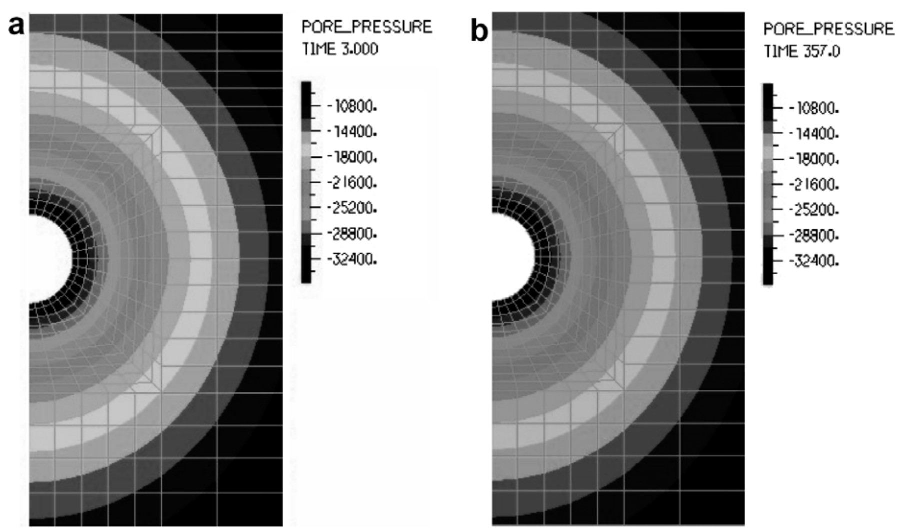

Fig. 12. Pore pressure distribution (shallow bore, $p_0 = 34.5$ kPa, permeability $k = 4.45e^{-6}$ Pa m^2/s) (a) at the initial stage and (b) at the steady flow condition.

An analytical equation provided by Staheli et al. (1998) is available to estimate the maximum allowable drilling fluid pressure. The equation is based on the classic perfect plasticity theory, and the maximum allowable drilling fluid pressure reads

$$\begin{aligned} p_{\max} &= u + p'_{\max} \\ &= u + (p'_{\mathrm{f}} + c \cdot \cot\phi) \cdot \left\{ \left(\frac{R_0}{R_{\mathrm{p,\,max}}} \right)^2 + Q \right\}^{\left(\frac{-\sin\phi}{1+\sin\phi}\right)} \\ &\quad - c \cdot \cot\phi \end{aligned} \tag{3}$$

In which u is the initial pore pressure that is taken as zero in this research. $p'_{\max}$ is the maximum allowable effective mud pressure. p'_{f} is the drilling mud pressure at which the first plastic deformation takes place. It is derived based on the rigid plastic theories:

$$p'_{\mathrm{f}} = \sigma'_0 \cdot (1 + \sin\phi) + c \cdot \cos\phi \tag{4}$$

σ'_0 is the initial effective soil stress at the center of the borehole. ϕ is the internal frictional angle. c is the soil cohesion. R_0 indicates the initial radius of the borehole. $R_{\mathrm{p,\,max}}$ signifies the radius of the plastic zone. Q, another mechanical parameter, can be obtained using

$$Q = \sigma'_0 \cdot \sin\phi + c \cdot \cos\phi / G \tag{5}$$

In Eq. (5), G represents the shear modulus. In Eqs. (3)–(5), stress and stress-like variables are measured in N/mm^2, and lengths are measured in millimeters. According to Conroy et al. (2002), $R_{\mathrm{p,\,max}}$ has a value of two thirds of the height of the soil cover over the borehole. Substituting in the above three equations all the necessary parameters we have used for the finite element analyses, an empirical maximum drilling mud pressure of 2.67 MPa is obtained, in contrast

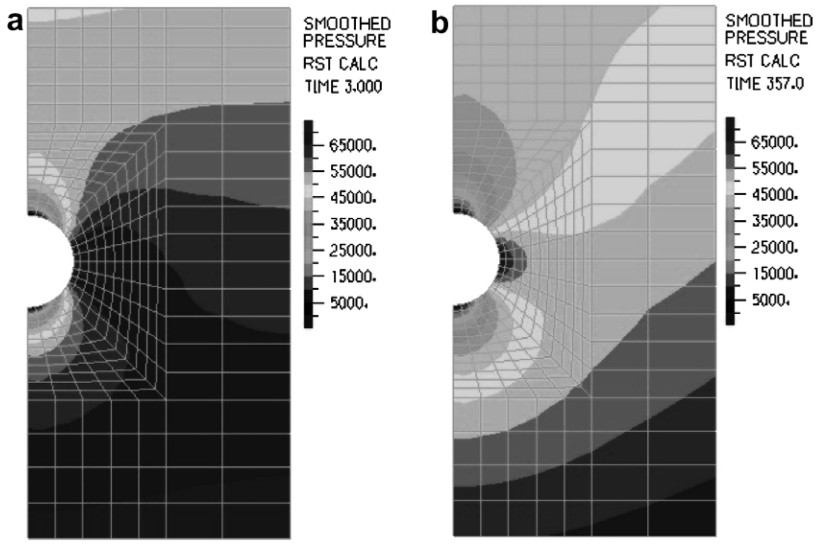

Fig. 13. Soil pressure distribution (shallow bore, $p_0 = 34.5$ kPa, permeability $k = 4.45e^{-11}$ Pa m^2/s) at the initial flow condition (a) and at the steady flow condition (b).

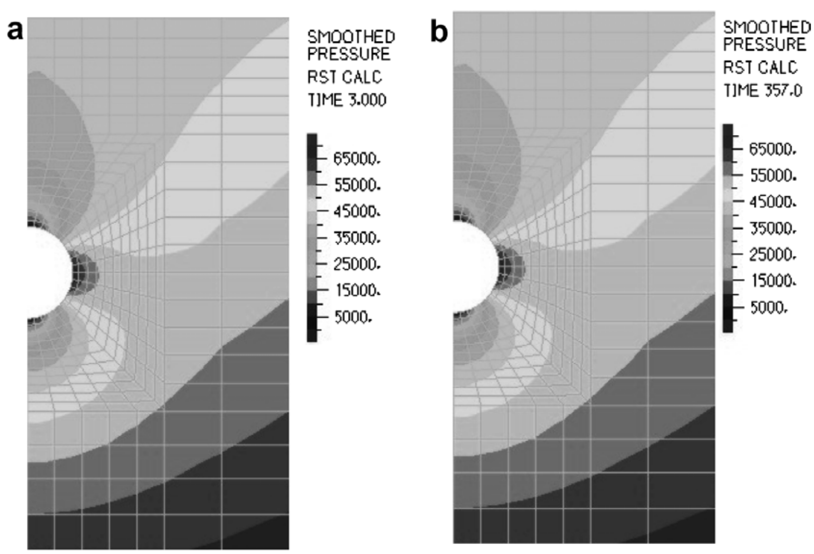

Fig. 14. Soil pressure distribution (shallow bore, $p_0 = 34.5$ kPa, permeability $k = 4.45e^{-6}$ Pa m^2/s) (a) at the initial stage and (b) at the steady flow condition.

to the rough value of 3.0 MPa gained from the finite element analysis, at which the soil bore wall collapsed because of hydraulic fracturing as the drilling fluid pressure is no longer able to be increased. Both the numerical and the closed-form solutions are close enough. However, corresponding to the critical drilling fluid pressure of 3.0 MPa, the plastic zone from the numerical analysis is approximately three times the diameter of the borehole, which is around 5.7 m, much less than the defined maximum plastic zone of about 20.3 m in the analytical equation.

The effect of soil cover is also investigated by changing the overburden depth to 6.10 m (shallow bore). Yielding zones and their development are plotted, in Fig. 16. Fig. 16a shows that the yield zone around the borehole is very limited if the drilling fluid pressure is between 88.3 kPa and 117.7 kPa. However, when the drilling fluid pressure is increased to 529.5 kPa, the yielding zone around the hole has been significantly enlarged. When the fluid pressure reaches 1.1 MPa, the radius of the yield zone is approximately 2.5 times the borehole radius, at

Table 4
Drilling fluid pressures corresponding to the solution times (deep bore)

Solution time	2	5	15
Drilling fluid pressure (kPa)	440.59	881.18	4405.9

Table 5
Drilling fluid pressures corresponding to the solution times (shallow bore)

Solution time	2	5	15
Drilling fluid pressure (kPa)	88.26	176.51	882.56

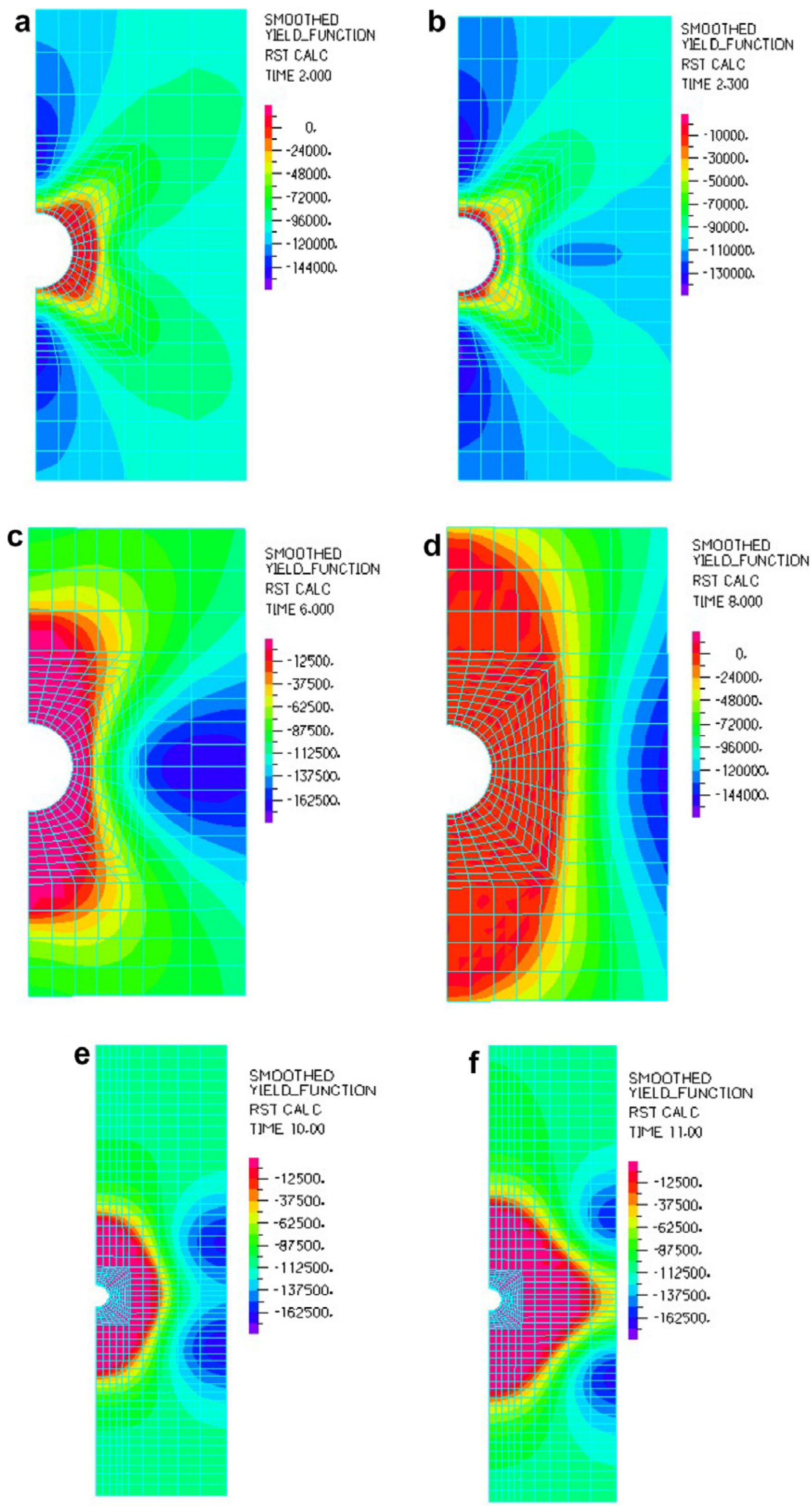

Fig. 15. Yield zones (red colored) corresponding to different drilling fluid pressures (deep bore) (a) 0.48 MPa, (b) 0.73 MPa, (c) 1.2 MPa, (d) 1.94 MPa (e) 2.64 MPa and (f) 3.0 MPa. (For interpretation of the references in color in this figure legend, the reader is referred to the web version of this article.)

which the hydraulic fracture failure occurs. The critical drilling fluid pressure from the analytical equation is calculated as 1.19 MPa, still very close to the numerical solution.

From all the presented solutions, some preliminary conclusions may be made. Even though a filter cake may be formed, a drilling fluid pressure maintained at a certain level is necessary to prevent the collapse of a borehole in

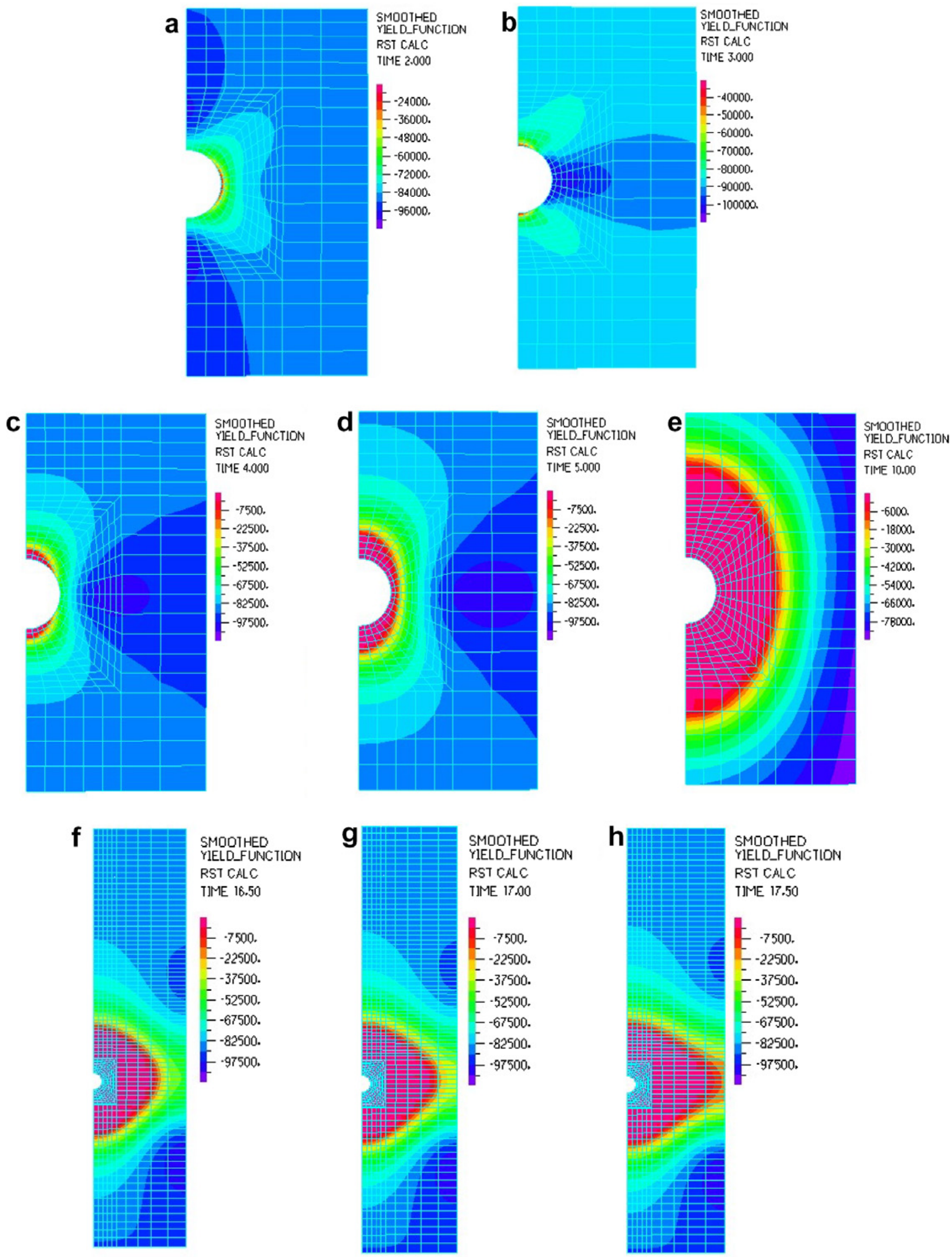

Fig. 16. Yield zones (red colored) around the borehole corresponding to different drilling fluid pressures (deep bore) (a) 88.26 kPa, (b) 117.68 kPa, (c) 147.09 kPa, (d) 176.51 kPa (e) 529.54 kPa, (f) 1.01 MPa, (g) 1.06 MPa and (h) 1.10 MPa. (For interpretation of the references in color in this figure legend, the reader is referred to the web version of this article.)

loose sands. A drilling fluid pressure at the initial earth pressure level of the soil mass appears to be the optimum choice to maintain borehole stability. Large fluid pressures may also lead to borehole collapse due to the expansion of the plastic yielding zone, namely so-called hydraulic fracturing in horizontal directional drilling. To obtain accurate numerical solutions, more efforts should be devoted to investigating the thickness and material properties of the filter cake.

5. Concluding remarks

The stability of a borehole in horizontal directional drilling has been studied in this paper with a particular focus